

Improved Simulation of an HVDC Test Case through Power-flow Initialization

N. Murray J. Arrillaga N.R. Watson Y.H. Liu

Abstract-- The steady state solutions derived from EMTP and power flow simulations differ due to the idealised and purely fundamental frequency system representation of the latter. This paper shows, however, that a preliminary power flow assessment of the operating condition can help to reduce substantially the initialization time of the EMTP solution. The test is carried out with reference to a new concept designed to exercise independent reactive power control in a multi-level CSC-HVDC scheme used for bulk power transmission from a remote power generating station.

Keywords: EMTDC, PSCAD, Power Flow, Multi-level conversion, HVDC Transmission.

I. INTRODUCTION

Electromagnetic Transients Programs (EMTP) and Power Flow are the two main simulation tools employed in the design and operation of ac-dc power systems. The purpose of a DC interconnection, a new control concept or a new converter configuration is to provide effective steady state power (active and reactive) transfers with acceptable voltage and current levels and waveforms. Therefore, the new project or ideas are first assessed by power flow simulation and only when the steady state objectives are met is the detailed design handed over to EMTP. The results of the power flow solution can also be used to initialize the EMTP studies. Moreover, the Power Flow and EMTP (on reaching the steady state) solutions can be used to cross validate each other.

However, the transition from Power Flow to EMTP is not straight forward, because of the idealised and purely fundamental frequency representation of the power flow solution.

An example of the complementary roles of Power Flow and EMTP is presented in this paper, with reference to a new concept used to provide more flexible control of the reactive power at the terminals of a long distance HVDC link connected to a remote generating plant.

The reason for the proposal is the lack of independent reactive power controllability of the multi-level schemes so far considered as possible alternatives to PWM-controlled VSC Transmission.

The new concept (referred to as multi-group firing-shift control) applies to self-commutating bipolar current-source

multi-level HVDC transmission with two or more converter groups at each terminal. The Multi-level Current Reinjection (MLCR) configuration is used as a basis for the test [1].

II. FIRING-SHIFT CONTROL OF THE CONVERTER GROUPS AT THE GENERATING STATION

Figure 1 shows a simplified equivalent of a bipolar self-commutating HVDC link connecting a large power station to an ac power system. The CSC converter stations consist of two twelve-pulse groups.

When the operating condition of the receiving end system requires an extra injection of reactive power from the converter, the converter firing angle increases. This action causes a dc voltage reduction and thus an increase of dc current. The latter, however, will be limited by a corresponding reduction of dc voltage at the sending end (implemented by an increase of firing angle) to maintain the specified power transfer. If, as is the case in conventional multi-group control, a common firing angle is used by the two groups, the extra reactive power injection at the receiving end will also result in an increase of reactive power injection at the sending end.

As the ac and dc voltages across the converter are related by the cosine of the firing angle, the sign of this angle does not affect the dc voltage level. In the proposed control, the dc voltage correction at the sending end in response to a reactive power increase at the receiving end is implemented by varying the firing angles of the two converter groups in opposite directions. Accordingly, one group (say group A) will advance the firing angle (i.e. inject more reactive power) and the other (say group B) delay the firing angle (i.e. absorb reactive power). This will maintain the converter operation at constant power factor.

The sending end converter groups can be set to operate with minimum firing angle (say zero) when the receiving end system requires minimum reactive power injection (i.e. for the case when the Short Circuit Ratio is largest). The generating station operates at its most efficient point when the generators are controlled to provide only active power to the link.

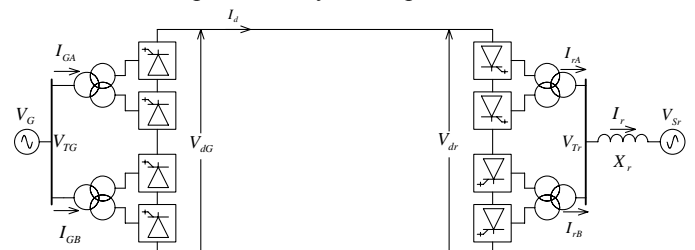


Figure 1. Simplified diagram of a DC link connecting a remote generating station

The authors are with the Electrical & Computer Engineering Department, University of Canterbury, Christchurch, 8020, New Zealand (e-mail: n.watson@elec.canterbury.ac.nz).

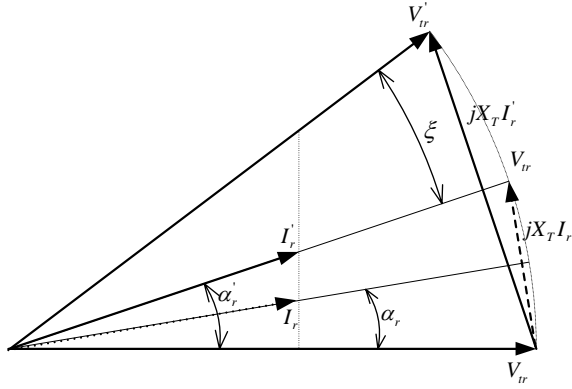


Figure 2. Effect of converter firing shift control on the relative position of the voltages and currents at the receiving end for an increased of the reactive power injection

III. INCORPORATION OF FIRING SHIFT CONTROL IN THE POWER-FLOW SOLUTION

The power-flow solution of an ac-dc-ac system is well documented [3] and a brief description of the algorithm is given in the Appendix. In a sequential solution, each iteration of the ac power flow updates the terminal voltages at the converter terminals and these are then used in the next dc iteration. To simplify the description, and verify the steady state performance, of the control algorithm proposed here to achieve reactive power independence at the terminals of the link, this section represents the ac systems as Thevenin equivalents (as shown in Fig. 1). In Figure 1 the receiving end double group converter is connected to an ac system represented by a voltage source (V_{Sr}) and a series reactance (X_r).

The relationship between the ac and dc currents across a single series connected group is [2]

$$I_r = k_m I_d \quad (1)$$

and the dc to ac voltage relationship across the double group converter

$$V_{dr} = 4(3\sqrt{2}/\pi)V_{Tr} \cos(\alpha_r) \quad (2)$$

The dc current can be expressed in terms of the specified power (which is normally controlled at the sending end of the link); therefore,

$$V_{dG} = V_{dr} + R_d \frac{P_{dG}^{sp}}{V_{dG}} \text{ or } V_{dG} = \frac{V_{dr} + \sqrt{V_{dr}^2 + 4R_d P_{dG}^{sp}}}{2} \quad (3)$$

Figure 2 illustrates two different operating conditions, determined by the value of the system impedance and, thus requiring different levels of reactive power at the receiving end. If both, the ac system voltage source (V_{Sr}) and the converter terminal voltage (V_{Tr}) are maintained constant (thus forcing the converter to share the reactive power provision equally with the ac system source), the following relationship applies to the phasor diagram of Figure 2:

$$(V_{Sr}/\sqrt{3})^2 - (V_{Tr}/\sqrt{3})^2 = X_r^2 I_r^2 - 2(V_{Tr}/\sqrt{3})X_r I_r \sin(\alpha_r) \quad (4)$$

The solution of Equations (1) to (4) provides the initial values of α_r , V_{dr} , V_{dG} , I_r

At the generating end the dc voltages of the individual converter groups are:

$$V_{dG}^A = 2(3\sqrt{2}/\pi)V_{TG} \cos(\delta\alpha) \quad (5a)$$

$$V_{dG}^B = 2(3\sqrt{2}/\pi)V_{TG} \cos(-\delta\alpha) \quad (5b)$$

where at all times

$$V_{dG}^A + V_{dG}^B = V_{dG}$$

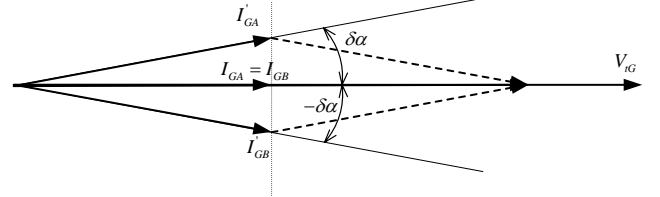


Figure 3. Effect of converter firing shift control on the generating plant currents following an increased in the reactive power injection at the receiving end

The firing shift ($\delta\alpha$), illustrated in Figure 3, ensures that the required value of V_{dG} can be achieved, while the generator continues to operate at unity power factor, without the need to alter the generator terminal voltage. This may be an important factor if the generating plant is also providing power to the local system.

A. Numerical Example

In the five level ($m = 5$) MLCR configuration [1] the value of k_m to be used in (1) is $k_m = 1.59$.

To simplify the description, let us assume that the receiving end voltage source (V_{Sr}) and converter terminal (V_{Tr}) line voltages are both equal to 1.02 pu (thus sharing equally the supply of reactive power); the specified dc power (P_{dG}) is 1pu and the series reactance (X_r) is .254 pu. Also, the resistance of the DC link (R_d) is 0.1 pu.

The following expressions apply (in per unit) for the specified operating conditions:

$$\text{From (1)} \quad I_{rA} = I_{rB} = (1.59) \frac{P_{dr}}{V_{dr}} = (1.59) \frac{1}{V_{dr}} \quad (6)$$

$$\text{From (2) and (6)} \quad \frac{1.59}{I_r} = 4(3\sqrt{2}/\pi)V_{Tr} \cos \alpha_r \quad (7)$$

Also the reactive power supplied by the converter (per phase) is half of the total requirement (a quarter per group), i.e.

$$Q_r^A = Q_r^B = (V_{Tr}/\sqrt{3})I_r \sin(\alpha_r) = \frac{1}{4} X_r (2I_r)^2$$

or

$$(V_{Tr} / \sqrt{3}) \sin(\alpha_r) = X_r I_r \quad (8)$$

The solution of (7) and (8) gives $\alpha_r = 7.2^\circ$ and $I_r = 0.291 pu$

and then from (6) $V_{dr} = 5.466 pu$

At the generating end, the DC voltage is calculated using (3) giving $V_{dG} = 5.485 pu$

Making $\delta\alpha = 0$ in Equation (5) the following expression applies to the group dc side voltage

$$(V_{dG} / 2) = 2(3\sqrt{2} / \pi)V_{TG}$$

or

$$V_{TG} = \frac{\pi}{12\sqrt{2}}V_{dG} = 1.0153 pu$$

If the receiving end series inductance is now increased by 50%, i.e. to $X_r = 0.381$,

the following values are derived from the above equations:

$$\alpha_r^{(1)} = 10.96^\circ, V_{dr}^{(1)} = 5.41, V_{dG}^{(1)} = 5.428, I_r^{(1)} = 0.294$$

Thus from Equation (5), to keep the generator terminal voltage constant (i.e. at 1.0153 pu), the phase shift at the sending end needs to be

$$\cos(\delta\alpha) = \frac{V_{dG}}{V_{TG}} \frac{\pi}{12\sqrt{2}} = \frac{5.419}{1.0146} \frac{\pi}{12\sqrt{2}} = .98976$$

or

$$\delta\alpha = \pm 8.25^\circ$$

which, as illustrated in Figure 3, permits the sending end converter to continue operating with unity power factor.

Repeating the calculations with a receiving end reactance of 0.508 p.u., yields the following results: $\alpha_r^{(2)} = 14.93^\circ, V_{dr}^{(2)} = 5.324, V_{dG}^{(2)} = 5.343, I_r^{(2)} = 0.2987, \partial\alpha_G^{(2)} = 13.06^\circ$

To minimize the value of $\delta\alpha$, and thus reduce the reactive power circulation between the converter groups; the generator terminal voltage can be reduced by excitation control. For instance in the numerical example above, the same dc voltage level (i.e. $V_{dG} = 5.428 pu$) could still be achieved with $\delta\alpha = 0$ if the generator voltage was reduced from 1.0146 to 1.003 pu. It would appear then that there is no need for firing shift control at the generating end. However, the firing shift will provide practically instantaneous controllability and then the slower excitation control will optimize the steady state operation. Moreover, the extra control would permit simplifying the generator excitation system or even the use of induction generators.

IV. ELECTROMAGNETIC SIMULATION

An attempt was first made to derive the steady state

characteristics purely by EMTDC simulation. This is highlighted in Figure 4, where the derivation of the required firing angle at the receiving end of the link to achieve the specified power flow condition (i.e. the equal sharing of reactive power between the ac system source and the converter) was achieved by a series of consecutive runs (each of a quarter of a second to ensure the steady state condition) for varying firing angles over a period of 10 seconds. As well as the firing angle variation, the figure plots the source and converter contributions to the reactive power, their crossing point representing the solution. This, of course, required a prohibited amount of computation.

Instead, the EMTDC simulation was constrained to an area around the steady state results obtained by the Power Flow solution. A direct transfer of the results from Power Flow to EMTDC is not possible because of the approximations made by the former, but they provided a good starting point for the dynamic simulation.

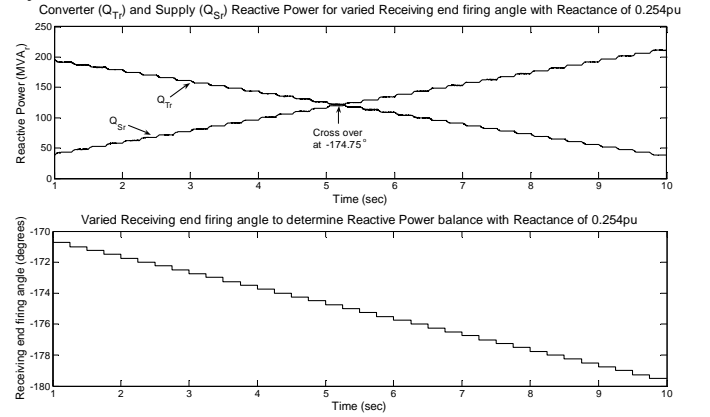


Figure 4. System and Converter Reactive power intersection at the receiving end with varied firing angle and system reactance of 0.254 pu

A. PSCAD/EMTDC model

The test case is based on a simplified HVDC link configuration, with the two interconnected systems represented as Thevenin circuits. Each terminal consists of two five-level MLCR converter groups as shown in Figure 1. The system is rated at 220kV, 1000MW at each end of the converter.

The firing angles calculated in Section 3 are selected as the initial control parameters for the sending and receiving ends. However at the sending end, instead of the 0° firing angle used in the power flow case, the minimum stable firing angle that could be used in the EMTDC simulation was $\pm 1.71^\circ$. This small amount of controller 'headroom' is needed to preserve the linearity in response to small perturbations in the transient simulation.

Also at the sending end, a minimum of 1.035pu voltage (instead of the 1.0153 value of the power flow solution) had to be set to achieve stable operation. This is understandable, due to the reduced power losses represented in the power flow as compared with the transient simulation model. The Power-flow solution assumes perfect conversion and considers only the effects of the fundamental supply frequency. The DC smoothing inductance is assumed infinite and lossless and the resistances of other ac side and dc line components are

specified by approximate per unit values.

Also, in the Power flow case, the entire Reinjection process is represented by a current conversion factor (1.59), which assumes perfect Reinjection (i.e. no account is taken of the switching and other component losses), whereas in the dynamic simulation environment these will vary depending on the operating conditions.

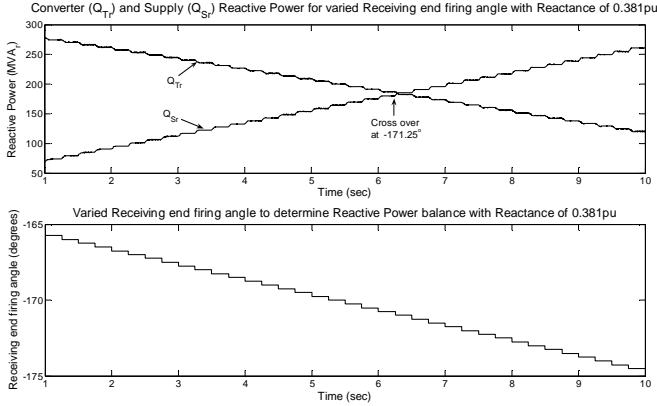


Figure 5. System and Converter Reactive power intersection at the receiving end with varied firing angle and system reactance of 0.381pu

B. Dynamic performance

The simulation uses a classical PI controller configured to modulate the sending and receiving end firing angles. A simplified version of the sending end controller is presented in Figure 6. The sending end is designed to control the real power, while the receiving end controller is configured to maintain the terminal voltage constant, and therefore balance reactive power between the converter and system.

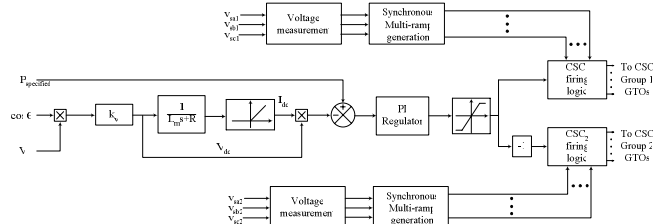


Figure 6 – Sending end Real power controller

The simulation is run for 2.5 seconds, with the receiving end system impedance modified in two large steps to simulate system reactances of 0.254, 0.381, and 0.508pu, at 0, 0.5 and 1.5s respectively. These large changes in system impedance are used to exaggerate the firing angle response; in practice, changes of this magnitude would only occur under fault conditions. Their effect on the sending end real and reactive powers are shown in Figures 9 & 10.

Using the Power Flow results as a guide allows the control system absolute boundaries to be set with reasonable confidence. This is particularly important because of the non-linear nature of the rectification and inversion processes using phase control [4]. If the converters are constrained to a relatively small operating range, say 20 – 30°, linear control systems provide a reasonable level of dynamic response [5]

A summary of the sending and receiving end firing angles in the power flow and EMTDC models, as well as their

relative errors are given in Table 1.

As with any simulation, there are limitations to the model's ability to replicate the real operating condition; necessarily approximations have to be made to make the model solvable and manageable. With EMTDC models, the most obvious of these is the discrete nature of the simulation, with a typical time step of 10µs used to represent the continuous domain.

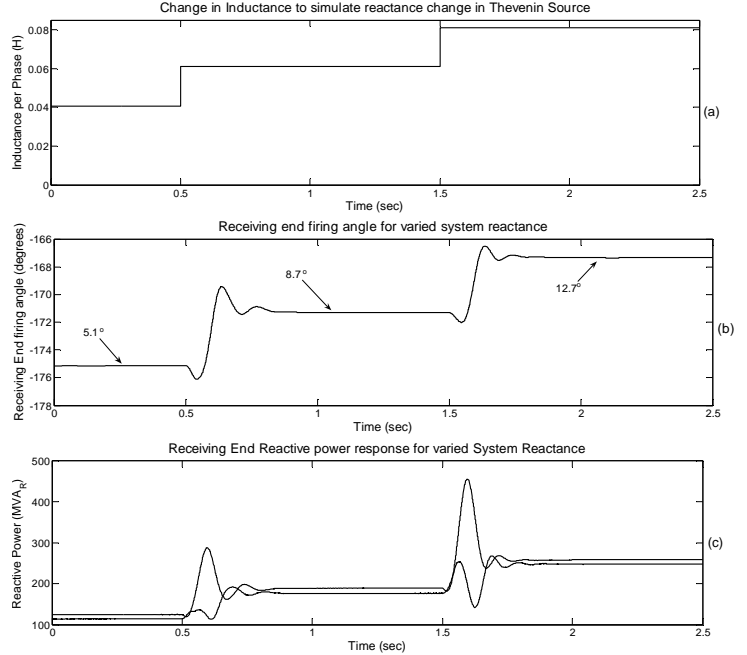


Figure 7. (a) – (c) Receiving end dynamic response to changes in system reactance

Table 1 – Comparison of Power Flow and EMTDC firing angle results

Case	System Reactance	Sending End Firing angle			Receiving end Firing angle		
		Power-Flow	EMTD C	Relative Error	Power Flow	EMTDC	Relative Error
(1)	0.254pu	7.2°	5.01°	30.4%	0.0°	1.71°	0.0%
(2)	0.381pu	10.96°	8.7°	20.6%	8.25°	7.9°	4.2%
(3)	0.508pu	14.93°	12.7°	14.9%	13.06°	12.1°	7.4%

In the proposed multi-level multi-group firing-shift control, as the sending end converter groups operate with different firing angles, circulating currents flow between the group transformers; these are not considered in the power flow solution. Also, in the EMTDC simulation, as the sending end groups are controlled to operate with equal and opposite firing angles, their currents are expected to sum perfectly to zero. However, due to the finite time steps used in EMTDC simulation, the exact zero crossing instants are interpolated, (in PSCAD trapezoidal interpolation is used) and slight variations in current will occur. For instance, although the sending end reactive power in the test case is expected to be zero, Figure 10 shows the presence of an average of 5MVA_r.

Often in EMTDC packages, the control system response is calculated every time step, which in the case of phase controlled HVDC systems, can actually lead to oscillation and

system instability [6]. To slow the control system down, filters are introduced, but there is trade off between a smooth response and suitable transient response. With the multi-group MLCR in this example, the sending end controller is filtered to provide an effective update rate of 1kHz, which is suitable for the main 50Hz bridges as well as the 5 level – 300Hz Reinjection schemes.

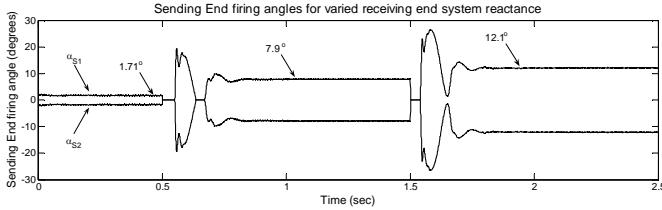


Figure 8. Sending end firing angle change in response to changes in receiving end system reactance.

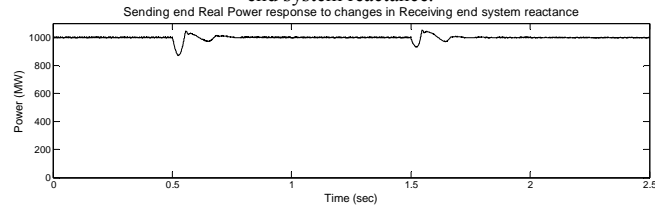


Figure 9. Sending end Real Power response to changes in receiving end system reactance

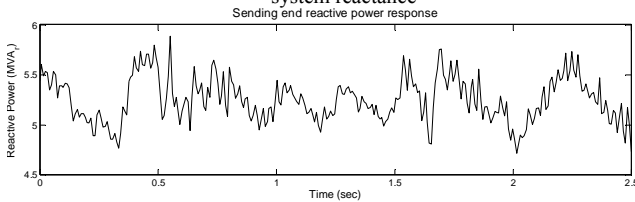


Figure 10. Sending end reactive power demands for varied receiving end system reactance

V. CONCLUSIONS

The relevance of the power flow solution as a preliminary tool to EMTF for the design of new ac-dc schemes has been the main aim of this contribution. As an example, the combination of PSCAD-EMTDC and Power Flow simulation has been used to test the ability of a new concept (referred to as double-group firing-shift control) to make current source multi-level HVDC Transmission more flexible in terms of reactive power controllability. This concept, applicable to bipolar schemes using two 12-pulse converter groups, has been shown to provide four quadrant power controllability at the two ends of the link. It may, therefore, be an interesting alternative to the conventional CSC and the recent and more flexible VSC technologies for bulk power HVDC transmission.

The use of power flow simulation to derive approximate initial conditions for the EMTF simulation has been shown to provide realistic information and reduce the computation task by at least an order of magnitude.

Also, on reaching the steady state the EMTF simulation have been shown to be sufficiently close to the Power Flow solution and thus provide cross-validation of the EMTDC and Power Flow results.

VI. REFERENCES

- [1] L.B. Perera, Y.H. Liu, N.R. Watson and J. Arrillaga, "Multi-level current reinjection in double-bridge self-commutated current source conversion", *Trans.IEEE on Power Delivery* Vol. 20, No. 2, April 2005, pp 984-991
- [2] J. Arrillaga, *HVDC Transmission* (2nd edition), IEE Power and Energy series No.29, London, 1998.
- [3] J. Arrillaga and N.R. Watson, 'Computer Modelling of Electrical Power Systems (second edition)', John Wiley and Sons, London, 2001
- [4] E. Uhlmann, 'Power Transmission by Direct Current', Springer-Verlag Berlin Heidelberg, New York, 1975
- [5] P. Kundur, 'Power System Stability and Control', McGraw-Hill Inc, New York, 1994
- [6] W. Forsythe and R. M. Goodall, *Digital Control, Fundamentals, Theory and Practice*, Macmillan Education Ltd, London, 1991

VII. BIOGRAPHY

Nick Murray received his B.E. (Hons) degree in electrical and electronic engineering from the University of Canterbury, Christchurch, New Zealand in 2001. Currently, he is pursuing his Ph.D. degree on the topic of Flexible Reactive Power Control in HVDC Converters at the University of Canterbury.

Jos Arrillaga received the B.E. degree in engineering from the University of Bilbao, Spain, in 1955, and the M.Sc., Ph.D., and D.Sc. degrees from the University of Manchester Institute of Science and Technology (UMIST), Manchester, U.K., in 1963, 1966, and 1981, respectively. He is a Fellow of the IEE, of the IEEE, and of the Academy of Science of New Zealand. He is now an Emeritus Professor at The University of Canterbury, New Zealand.

Neville R. Watson received his B.E. (Hons) and Ph.D. degrees in electrical and electronic engineering from the University of Canterbury (New Zealand) where he is now a Associate Professor. His interests include power quality, steady-state and dynamic analysis of ac/dc power systems.

Yonghe Liu received the M.E. degree in automation from The Chinese Science Academy, Beijing, China and Ph.D. degree from the University of Canterbury, New Zealand. He is a Professor at Inner Mongolia University of Technology, China and an EPCA Trust Fellow at The University of Canterbury, New Zealand.

VIII. APPENDIX

The operating state of a combined ac-dc power system is defined by the vector

$$[\bar{V}, \bar{\theta}, \bar{x}]^T$$

where

\bar{V} - is a vector of the voltage magnitudes at all a.c. system busbars.

$\bar{\theta}$ - is a vector of the angles at all a.c. system busbars (except the reference bus which is assigned $\theta = 0$).

\bar{x} - is the vector of d.c. variables.

In the Newton-Raphson load flow solution the equations that relate to the a.c. system variables are derived from the specified a.c. system operating conditions. The only modification required to the usual real and reactive power mismatches are in the interface equations at the converter terminal busbars, i.e.

$$P_{term}^{sp} - P_{term}(ac) - P_{term}(dc) = 0 \quad (A1)$$

$$Q_{term}^{sp} - Q_{term}(ac) - Q_{term}(dc) = 0 \quad (A2)$$

where

$P_{term}(ac)$ and $Q_{term}(ac)$ are the injected active and reactive powers at the terminal busbar as a function of the a.c. system variables.

P_{term}^{sp} represents an a.c. system load at the converter bus.

The injected powers $Q_{term}(dc)$ and $P_{term}(dc)$ are functions of the converter a.c. terminal busbar voltage and of the d.c. system variables, i.e.

$$P_{term(dc)} = V_d \cdot I_d \quad (A3)$$

and

$$Q_{term(dc)} = V_{term} \cdot I_p \cdot \sin(\alpha) \quad (A4)$$

The equations derived from the specified a.c. system conditions may, therefore, be summarised as:

$$\begin{bmatrix} \Delta \bar{P}(\bar{V}, \bar{\theta}) \\ \Delta \bar{P}_{term}(\bar{V}, \bar{\theta}, \bar{x}) \\ \Delta \bar{Q}(\bar{V}, \bar{\theta}) \\ \Delta \bar{Q}_{term}(\bar{V}, \bar{\theta}, \bar{x}) \end{bmatrix} = 0 \quad (A5)$$

where the mismatches at the converter terminal busbars are indicated separately.

A further set of independent equations are derived from the d.c. system conditions. These equations, designated by the vector,

$$\bar{R}(V_{term}, \bar{x})_k = 0 \quad (A6)$$

where vector \bar{R} and \bar{x} are the firing angles of the two groups of the converter station.

In the Fast Decoupled power flow (the most commonly used algorithm)[book] and a sequential solution, the following three equations need to be solved iteratively to convergence.

$$[\Delta \bar{P} / \bar{V}] = [B'] [\Delta \bar{\theta}] \quad (A7)$$

$$[\Delta \bar{Q} / \bar{V}] = [B''] [\Delta \bar{V}] \quad (A8)$$

$$[\bar{R}] = [A] [\Delta \bar{x}] \quad (A9)$$

where (A7) and (A8) are those of the standard ac system Fast Decoupled algorithm with the dc modelled as a real and reactive power injection at the appropriate terminal busbar. Equation (A9) is the dc solution, with the ac system modelled as a constant voltage at the converter terminals.

This iteration sequence is as follows:

- (i) Calculate $\Delta \bar{P} / \bar{V}$, solve equation (A7) and update $\bar{\theta}$.
- (ii) Calculate $\Delta \bar{Q} / \bar{V}$, solve equation (A8) and update

\bar{V} .

(iii) Calculate d.c. residuals, \bar{R} , solve equation (A9) and update \bar{x} .

(iv) Return to (i).